Chemical Engineering Journal 100 (2004) 1–9

Chemical Engineering Journal

www.elsevier.com/locate/cej

Internal liquid circulation in annulus sparged internal loop airlift contactors

Porntip Wongsuchoto, Prasert Pavasant*

Department of Chemical Engineering, Faculty of Engineering, Chulalongkorn University, Bangkok 10330, Thailand

Received 7 June 2003; accepted 8 November 2003

Abstract

Measurement of liquid velocities in downcomer and riser of the annulus sparged internal loop airlift contactor (ALC) revealed that there was an unbalance fluid flow in the system. This was due to the existence of the internal liquid circulation in the riser of the ALC. A mathematical model based on material and energy conservation principals was then introduced to determine the extent of this internal liquid circulation. It was shown that the internal liquid circulation was affected predominantly by the superficial gas velocity (u_{sg}) and the ratio between downcomer to riser cross-sectional areas (A_d/A_r) of the ALC. An increase in u_{sg} gave rise to the down-flow liquid flowrate in the riser, but on the other hand, reduced the fraction of down-flow area in riser. A_d/A_r was found not to significantly influence the fraction of down-flow and up-flow areas but small A_d/A_r tended to increase the down-flow velocity in the riser.

Keywords: Airlift contactor; Internal liquid circulation; Liquid circulation; Mathematical model; Material conservation principal; Energy conservation principal

1. Introduction

A defined cyclic liquid circulation pattern between riser and downcomer of airlift contactor (ALC) is an important characteristic which distinguishes them from other types of gas–liquid contacting devices. In addition to the primary liquid circulation between riser and downcomer, there also exists a secondary liquid circulation usually known as "internal liquid circulation" which takes place locally either in riser or downcomer. This type of flow is similar to that which dominates the behavior of liquid in bubble columns [1–5]. In the work by Jones [6], it was found that the measurement of liquid velocity in the draft tube sparged ALC did not correspond well with the model prediction. This was concluded to be attributed to the existence of internal liquid circulation in riser. Shortly after that, Merchuk and Siegel [7] observed that the up-flow pattern in riser was occasionally suppressed and became more turbulent, especially at high gas flowrate. They concluded that there must be internal liquid circulation taking place in riser of the ALC.

The development of mathematical models for ALCs often emphasized that internal liquid circulation must have taken place within the system. For instance, Calvo and Letón [8] incorporated the turbulent energy dissipation due to the internal liquid circulation in the riser into their energy conservation based model and found that their simulation results agreed well with a wide range of reported experimental data. This energy dissipation was considered similar to that occurred in bubble columns. Wachi et al. [9] stated that there were fluid flow contractions at the entrances of riser and downcomer, which were dependent markedly on the draft tube diameter, or rather, the ratio between cross-sectional areas of downcomer and riser (A_d/A_r). It was reported in this article that the increase in draft tube diameter for a draft tube sparged ALC resulted in a relatively larger flow contraction at the riser entrance. In downcomer, the increase in draft tube diameters induced high liquid velocity which reduced the flow contraction at the downcomer entrance.

Despite the awareness of this type of liquid flow in the ALC, the quantitative and qualitative analyses of this type of flow in ALC have not been given adequate attention and, hence, its role in characterizing the behavior of ALCs is unclear. It was therefore the aim of this work to investigate the local fluid flow behavior within the annulus sparged internal loop airlift contactor. The effects of geometrical and operational parameters, i.e. downcomer to riser cross-sectional area ratio and superficial gas velocity,

* Corresponding author. Tel.: +662-218-6870; fax: +662-218-6877.
E-mail address: prasert.p@chula.ac.th (P. Pavasant).

1385-8947/$ – see front matter
doi:10.1016/j.cej.2003.11.003

Nomenclature

A	cross-sectional area (m^2)
D_0	inside diameter of outer column (m)
D_i	inside diameter of draft tube (m)
D_{i0}	outside diameter of draft tube (m)
e_v	friction loss factor
$\hat{E}_v$	friction loss or the rate at which mechanical energy is irreversibly converted to thermal energy (W)
f	friction factor
g	gravitational acceleration (m^2/s)
ΔH	distance between pressure measurement points (m)
H	height (m)
Δh	difference in elevation between planes '1' and '2' (m)
L	length (m)
ΔP	hydrostatic pressure difference between two measuring points (N/m^2)
P	pressure (Pa)
Q	volumetric flowrate (m^3/s)
Q_{Gm}	gas molar flowrate (mol/s)
Re	Reynolds number (–)
R_h	mean hydraulic radius (m)
u_L	superficial liquid velocity (m/s)
u_{sg}	superficial gas velocity (m/s)
v	velocity (m/s)
$\dot{w}$	mass flowrate (kg/s)
$\hat{W}$	rate at which the system performs mechanical work on its surroundings (W)

Greek letters

ε	holdup
μ	viscosity (kg/m s)
ρ	density (kg/m^3)

Subscripts

b	bottom
D	dispersion or downcomer
d	downcomer
dn	down-flow
dt	draft tube
G	gas
L	liquid
R, r	riser
t	top
up	up-flow

respectively, were included in the study. The model for predicting proportion of internal liquid circulation based on material and mechanical energy conservation was proposed.

2. Mathematical model with internal liquid circulation

The existing of internal liquid circulation within riser (annular section) was evaluated based on the material and energy conservation principals. A mathematical model into which the internal liquid circulation is incorporated was developed based on the following assumptions.

1. Steady-state conditions.
2. One-directional isothermal flow.
3. Uniform gas holdups in up-flow region of riser and downcomer along the axial direction.
4. No gas recirculation in down-flow area of riser ($\varepsilon_{Gr,dn} = 0$) [10].
5. Negligible interaction between the gas phase and the wall, i.e. negligible influence of the gas phase on the friction [11].
6. Negligible gravitational force for gas bubbles.

2.1. Steady-state macroscopic mass balance (continuity equation)

A simple form of continuity equation for the case where the liquid mass flow in downcomer was equal to that in riser, i.e. internal liquid circulation was assumed not to exist, can be written as

$$v_{Ld} A_d (1 - \varepsilon_{Gd}) = v_{Lr} A_r (1 - \varepsilon_{Gr}) \quad (1)$$

To account for the existing of internal liquid circulation in riser, there must be a fraction of riser that allowed a down-flow of liquid, in addition to the conventional up-flow direction, as illustrated in a schematic diagram of liquid flow in Fig. 1. In this figure, there was a flow of liquid entering the downcomer at plane # '1', and leaving the system at plane #

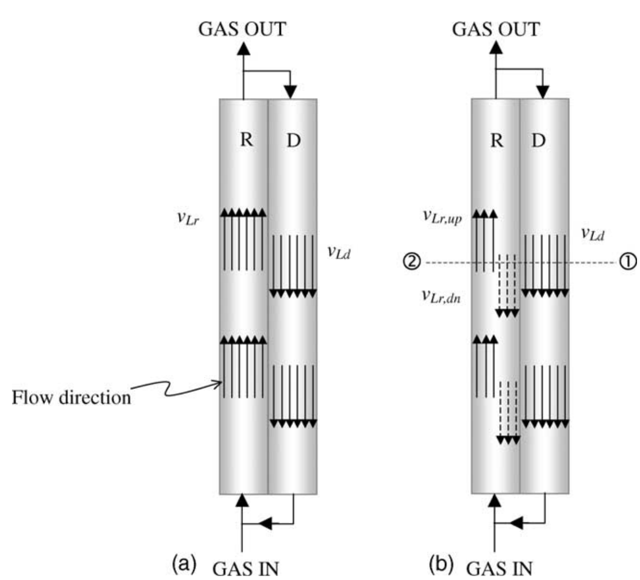

Fig. 1. Schematic diagram of liquid flow in ALC: (a) conventional model for liquid flow; (b) model for liquid flow in ALC with internal liquid circulation.

'2' in the riser. The liquid flow in riser was divided into two distinct regions: the uniformly distributed bubble region in the inner annular region and the bubble-free in outer annular region ($\varepsilon_{\mathrm{Gr,dn}} = 0$). It was assumed that the bubble region was also uniform in gas holdup. For this case, the RHS of the mass balance of liquid phase, Eq. (1), should include the liquid recirculation term which can be expressed as

$$v_{\mathrm{Ld}} A_{\mathrm{d}}(1-\varepsilon_{\mathrm{Gd}}) = v_{\mathrm{Lr,up}} A_{\mathrm{r,up}}(1-\varepsilon_{\mathrm{Gr,up}}) - v_{\mathrm{Lr,dn}} A_{\mathrm{r,dn}}(1-\varepsilon_{\mathrm{Gr,dn}}) \qquad (2)$$

where $v_{\mathrm{Lr,up}}$ is the riser liquid velocity in up-flow region which occupies the area of $A_{\mathrm{r,up}}$, and $v_{\mathrm{Lr,dn}}$ is the riser liquid velocity in down-flow region which occupies the area of $A_{\mathrm{r,dn}}$. The negative term on the RHS of Eq. (2) accounts for down-flow liquid in the riser. The total area of riser is equal to the sum of the up-flow area ($A_{\mathrm{r,up}}$) and down-flow area ($A_{\mathrm{r,dn}}$)

$$A_{\mathrm{r,up}} + A_{\mathrm{r,dn}} = A_{\mathrm{r}} \qquad (3)$$

Substitute $A_{\mathrm{r,up}}$ from Eq. (3) into Eq. (2) gives

$$v_{\mathrm{Ld}} A_{\mathrm{d}}(1-\varepsilon_{\mathrm{Gd}}) = v_{\mathrm{Lr,up}}(A_{\mathrm{r}} - A_{\mathrm{r,dn}})(1-\varepsilon_{\mathrm{Gr,up}}) - v_{\mathrm{Lr,dn}} A_{\mathrm{r,dn}}(1-\varepsilon_{\mathrm{Gr,dn}}) \qquad (4)$$

2.2. Steady state macroscopic energy balance

The energy balance can be expressed using the Bernoulli equation [12]

$$0 = \Delta\frac{1}{2}\langle\bar{v}\rangle^2 + g\Delta h + \int_{P_1}^{P_2}\frac{1}{\rho}\,\mathrm{d}P + \hat{W} + \hat{E}_{\mathrm{v}} \qquad (5)$$

where $\hat{W}$ is the rate at which the system performs mechanical work on its surroundings and $\hat{E}_{\mathrm{v}}$ the friction loss or the rate at which mechanical energy is irreversibly converted to thermal energy.

The energy input to any ALCs obtained from potential energy due to isothermal gas expansion is

$$\hat{W} = \frac{P_{\mathrm{b}}}{\rho_{\mathrm{G}}}\ln\left(1 + \frac{\rho_{\mathrm{L}} g H_{\mathrm{L}}}{P_{\mathrm{t}}}\right) \qquad (6)$$

The friction losses ($\hat{E}_{\mathrm{v}}$) are composed of frictions from all sections of straight conduits and all fittings including friction losses at gas–liquid interface both in riser and downcomer which could be calculated from Eq. (7).

$$\hat{E}_{\mathrm{v}} = \sum_i \hat{E}_{\mathrm{v}i} \qquad (7)$$

Substitute Eqs. (6) and (7) into Eq. (5) yields

$$0 = \Delta\frac{1}{2}\langle\bar{v}\rangle^2 + g\Delta h + \int_{P}^{P_2}\frac{1}{\rho}\,\mathrm{d}P + \frac{P_{\mathrm{b}}}{\rho_{\mathrm{G}}}\ln\left(1 + \frac{\rho_{\mathrm{L}} g H_{\mathrm{L}}}{P_{\mathrm{t}}}\right) + \sum_i \hat{E}_{\mathrm{v}i} \qquad (8)$$

Usually the energy term due to the gas flow was found negligible when compared to the energy term due to liquid flow [11,13], and this energy term was not considered in this work. Thus, the energy balance of liquid phase, Eq. (8), can be rewritten as

$$\begin{aligned} 0 = {} & \frac{1}{2}\dot{w}_{\mathrm{Ld}} v_{\mathrm{Ld}}^2 - \frac{1}{2}\dot{w}_{\mathrm{Lr,up}} v_{\mathrm{Lr,up}}^2 + \frac{1}{2}\dot{w}_{\mathrm{Lr,dn}} v_{\mathrm{Lr,dn}}^2 \\ & - \dot{w}_{\mathrm{Ld}} g h_{\mathrm{d}} + \dot{w}_{\mathrm{Lr,up}} g h_{\mathrm{r}} - \dot{w}_{\mathrm{Lr,dn}} g h_{\mathrm{r}} \\ & + \int_{P_1}^{P_2}\left(\frac{\dot{w}_{\mathrm{Ld}}}{\rho_{\mathrm{L}}} + \frac{\dot{w}_{\mathrm{Lr,up}}}{\rho_{\mathrm{L}}} + \frac{\dot{w}_{\mathrm{Lr,dn}}}{\rho_{\mathrm{L}}} + \frac{\dot{w}_{\mathrm{Gr,up}}}{\rho_{\mathrm{G}}}\right)\mathrm{d}P \\ & + Q_{\mathrm{G}} P_{\mathrm{b}} \ln\left(1 + \frac{\rho_{\mathrm{L}} g H_{\mathrm{L}}}{P_{\mathrm{t}}}\right) + \sum_i \hat{E}_{\mathrm{v}i} \end{aligned} \qquad (9)$$

Substitute $\dot{w} = \rho_{\mathrm{L}} v_{\mathrm{L}} A(1-\varepsilon_{\mathrm{G}})$ into Eq. (9) yields

$$\begin{aligned} 0 = {} & \frac{1}{2}\rho_{\mathrm{L}} A_{\mathrm{d}}(1-\varepsilon_{\mathrm{Gd}}) v_{\mathrm{Ld}}^3 - \frac{1}{2}\rho_{\mathrm{L}} A_{\mathrm{r,up}}(1-\varepsilon_{\mathrm{Gr,up}}) v_{\mathrm{Lr,up}}^3 \\ & + \frac{1}{2}\rho_{\mathrm{L}} A_{\mathrm{r,dn}}(1-\varepsilon_{\mathrm{Gr,dn}}) v_{\mathrm{Lr,dn}}^3 - \rho_{\mathrm{L}} A_{\mathrm{d}}(1-\varepsilon_{\mathrm{Gd}}) v_{\mathrm{Ld}} g h_{\mathrm{d}} \\ & + \rho_{\mathrm{L}} A_{\mathrm{r,up}}(1-\varepsilon_{\mathrm{Gr,up}}) v_{\mathrm{Lr,up}} g h_{\mathrm{r}} \\ & - \rho_{\mathrm{L}} A_{\mathrm{r,dn}}(1-\varepsilon_{\mathrm{Gr,dn}}) v_{\mathrm{Lr,dn}} g h_{\mathrm{r}} \\ & + \int_{P_1}^{P_2}\left[A_{\mathrm{d}}(1-\varepsilon_{\mathrm{Gd}}) v_{\mathrm{Ld}} + A_{\mathrm{r,up}}(1-\varepsilon_{\mathrm{Gr,up}}) v_{\mathrm{Lr,up}} \right. \\ & \left. + A_{\mathrm{r,dn}}(1-\varepsilon_{\mathrm{Gr,dn}}) v_{\mathrm{Lr,dn}} + A_{\mathrm{r,up}}\varepsilon_{\mathrm{Gr,up}} v_{\mathrm{Gr,up}}\right]\mathrm{d}P \\ & + Q_{\mathrm{G}} P_{\mathrm{b}} \ln\left(1 + \frac{\rho_{\mathrm{L}} g H_{\mathrm{L}}}{P_{\mathrm{t}}}\right) + \sum_i \hat{E}_{\mathrm{v}i} \end{aligned} \qquad (10)$$

Energy dissipations ($\hat{E}_{\mathrm{v}}$) taken into consideration in this work were those due to frictions in conduits, i.e. riser, downcomer, top and bottom sections, $\hat{E}_{\mathrm{vr}}$, $\hat{E}_{\mathrm{vd}}$, $\hat{E}_{\mathrm{vt}}$ and $\hat{E}_{\mathrm{vb}}$, respectively, and frictions from the movement of gas bubbles in liquid (at gas–liquid interface) in the riser and downcomer, $\hat{E}_{\mathrm{vsr}}$, $\hat{E}_{\mathrm{vsd}}$, respectively. The energy dissipations due to frictions in conduits can be calculated from:

$$\hat{E}_{\mathrm{v}i} = \sum_i\left(\frac{1}{2}\rho_{\mathrm{L}} A(1-\varepsilon_{\mathrm{G}}) v_{\mathrm{L}}^3 \frac{L}{R_{\mathrm{h}}} f\right)_i + \sum_i\left(\frac{1}{2}\rho_{\mathrm{L}} A(1-\varepsilon_{\mathrm{G}}) v_{\mathrm{L}}^3 e_{\mathrm{v}}\right)_i \qquad (11)$$

where $\sum_i ((1/2)\rho_{\mathrm{L}} A(1-\varepsilon_{\mathrm{G}}) v_{\mathrm{L}}^3 (L/R_{\mathrm{h}}) f)_i$ is the sum on all friction losses in sections of straight conduits such as riser and downcomer, and $\sum_i ((1/2)\rho_{\mathrm{L}} A(1-\varepsilon_{\mathrm{G}}) v_{\mathrm{L}}^3 e_{\mathrm{v}})_i$ represents the sum of friction losses at top and bottom sections. However, the friction loss can usually be neglected for the open liquid surface such as at the top section [14,15]. Eq. (11) can be written in a simple form as follows:

$$\hat{E}_{\mathrm{v}i} = \sum_i\left(\frac{1}{2}\rho_{\mathrm{L}} A(1-\varepsilon_{\mathrm{G}}) v_{\mathrm{L}}^3 \left(\frac{L}{R_{\mathrm{h}}} f + e_{\mathrm{v}}\right)\right)_i \qquad (12)$$

where R_{h} is the mean hydraulic radius and e_{v} the friction loss factor, and f the friction factor which is a function of

Reynolds number according to [12]

$$f = \frac{16}{Re} \quad \text{for } Re < 2100;$$
$$f = \frac{0.0791}{Re^{1/4}} \quad \text{for } 2100 < Re < 10^5 \tag{13}$$

where Re is Reynolds number defined as Eq. (14) (for the annular section of the ALC).

$$Re = \frac{4R_\mathrm{h}\langle v_\mathrm{L}\rangle \rho_\mathrm{L}}{\mu_\mathrm{L}} \tag{14}$$

In the determination of these energy dissipations, the friction loss factor (e_v) for the bottom section of the contactor was assumed to be 1.8 for the two 90° elbow (rounded) connectors [12]. The energy dissipation due to the friction in the riser (annulus section) was calculated in the same fashion as that in downcomer. However, there existed two distinct flow behaviors in the riser: up-flow and down-flow due to internal liquid recirculation. Hence, the total energy dissipation from frictions in conduits becomes

$$\begin{aligned}\hat{E}_\mathrm{v} &= \frac{1}{2}\rho_\mathrm{L} A_\mathrm{d}(1-\varepsilon_\mathrm{Gd})v_\mathrm{Ld}^3\left(\frac{L_\mathrm{d}}{R_\mathrm{hd}} f_\mathrm{d} + e_\mathrm{v}\right)\\ &\quad + \frac{1}{2}\rho_\mathrm{L} A_\mathrm{r,up}(1-\varepsilon_\mathrm{Gr,up})v_\mathrm{Lr,up}^3\left(\frac{L_\mathrm{r,up}}{R_\mathrm{hr,up}} f_\mathrm{r,up}\right)\\ &\quad + \frac{1}{2}\rho_\mathrm{L} A_\mathrm{r,dn}(1-\varepsilon_\mathrm{Gr,dn})v_\mathrm{Lr,dn}^3\left(\frac{L_\mathrm{r,dn}}{R_\mathrm{hr,dn}} f_\mathrm{r,dn}\right)\end{aligned} \tag{15}$$

The energy dissipation due to frictions from the movement of gas bubbles in liquid, $\hat{E}_\mathrm{vsr}$ and $\hat{E}_\mathrm{vsd}$, can be calculated from [16,17]:

$$\hat{E}_\mathrm{vsr} + \hat{E}_\mathrm{vsd} = v_\mathrm{s}\rho_\mathrm{L} g H_\mathrm{Dr}\varepsilon_\mathrm{Gr} + \rho_\mathrm{L} g H_\mathrm{Dd} u_\mathrm{Ld} A_\mathrm{d}\varepsilon_\mathrm{Gd} \tag{16}$$

Substitute Eqs. (15) and (16) into Eq. (10) yields

$$\begin{aligned}0 &= A_\mathrm{d}(1-\varepsilon_\mathrm{Gd})v_\mathrm{Ld}^3 - A_\mathrm{r,up}(1-\varepsilon_\mathrm{Gr,up})v_\mathrm{Lr,up}^3\\ &\quad + A_\mathrm{r,dn}(1-\varepsilon_\mathrm{Gr,dn})v_\mathrm{Lr,dn}^3 - 2A_\mathrm{d}(1-\varepsilon_\mathrm{Gd})v_\mathrm{Ld} g h_\mathrm{d}\\ &\quad + 2A_\mathrm{r,up}(1-\varepsilon_\mathrm{Gr,up})v_\mathrm{Lr,up} g h_\mathrm{r}\\ &\quad - 2A_\mathrm{r,d}(1-\varepsilon_\mathrm{Gr,dn})v_\mathrm{Lr,dn} g h_\mathrm{r}\\ &\quad + \frac{2}{\rho_\mathrm{L}}\int_{P_1}^{P_2}[A_\mathrm{d}(1-\varepsilon_\mathrm{Gd})v_\mathrm{Ld}]\,\mathrm{d}P\\ &\quad + \frac{2}{\rho_\mathrm{L}}\int_{P_1}^{P_2}[A_\mathrm{r,up}(1-\varepsilon_\mathrm{Gr,up})v_\mathrm{Lr,up}]\,\mathrm{d}P\\ &\quad + \frac{2}{\rho_\mathrm{L}}\int_{P_1}^{P_2}[A_\mathrm{r,dn}(1-\varepsilon_\mathrm{Gr,dn})v_\mathrm{Lr,dn}]\,\mathrm{d}P\\ &\quad + \frac{2}{\rho_\mathrm{L}}\int_{P_1}^{P_2}[A_\mathrm{r,up}\varepsilon_\mathrm{Gr,up} v_\mathrm{Gr,up}]\,\mathrm{d}P + \frac{2Q_\mathrm{G}P_\mathrm{b}}{\rho_\mathrm{L}}\\ &\quad \times \ln\left(1+\frac{\rho_\mathrm{L} g H_\mathrm{L}}{P_\mathrm{t}}\right) - A_\mathrm{d}(1-\varepsilon_\mathrm{Gd})v_\mathrm{Ld}^3\left(\frac{L_\mathrm{d}}{R_\mathrm{hd}} f_\mathrm{d} + e_\mathrm{v}\right)\\ &\quad - A_\mathrm{r,up}(1-\varepsilon_\mathrm{Gr,up})v_\mathrm{Lr,up}^3\left(\frac{L_\mathrm{r,up}}{R_\mathrm{hr,up}} f_\mathrm{r,up}\right)\\ &\quad - A_\mathrm{r,dn}(1-\varepsilon_\mathrm{Gr,dn})v_\mathrm{Lr,dn}^3\left(\frac{L_\mathrm{r,dn}}{R_\mathrm{hr,dn}} f_\mathrm{r,dn}\right)\\ &\quad + 2gH_\mathrm{Dd}u_\mathrm{Ld}A_\mathrm{d}\varepsilon_\mathrm{Gd} + 2v_\mathrm{s} g H_\mathrm{Dr}\varepsilon_\mathrm{Gr}\end{aligned} \tag{17}$$

To solve these equations, certain parameters including downcomer liquid velocity (v_Ld), downcomer gas holdup (ε_Gd), liquid velocity in up-flow region of riser ($v_\mathrm{Lr,up}$), gas holdup in up-flow region of riser ($\varepsilon_\mathrm{Gr,up}$), and gas holdup in down-flow region of riser ($\varepsilon_\mathrm{Gr,dn}$) had to be known in a priori, and for this work, they were determined experimentally as described below.

3. Experimental

3.1. Apparatus

A schematic diagram of experimental setup for this work is shown in Fig. 2. Experiments were carried out in a transparent cylindrical column with a height of 1.2 m and a diameter, D_0, of 0.137 m. The column was equipped with pressure taps at every 0.1 m along the contactor height for the measurement of pressure drop, ΔP, which was used to determine the riser gas holdup, ε_Gr. A draft tube with a height of 1 m was inserted into the column where a clearance between the column base and the end of the draft tube was fixed at 5 cm. The ratio between cross-sectional areas of downcomer and riser was altered by changing draft tube diameter of which dimension is provided in Table 1. The unaerated water level was controlled at 3 cm above the top of these draft tubes. Experiments were operated in a semi-batch operation where a continuous air flow was supplied through a perforated ring sparger into the water-filled column. Air flowrate was controlled by a calibrated rotameter to give

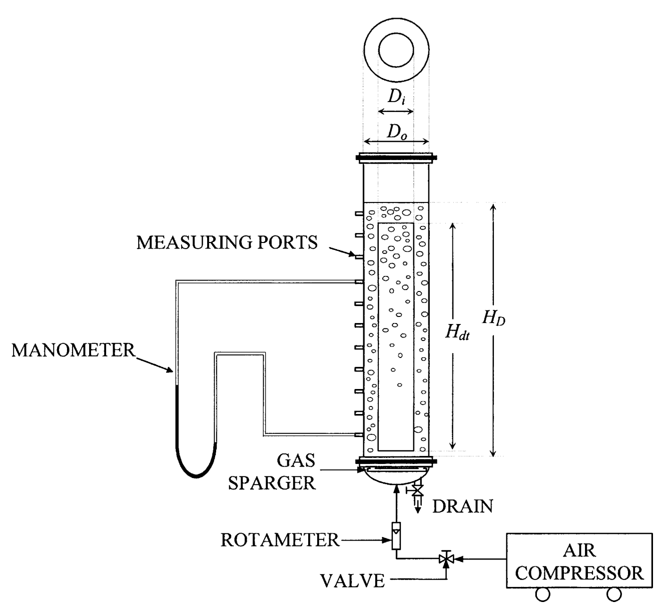

Fig. 2. Experimental apparatus of the concentric internal loop airlift contactor.

Table 1
Specification of ALCs used in this work

ALC	D_i (m)	D_{i0} (m)	A_d/A_r
ALC-1	0.034	0.040	0.067
ALC-2	0.074	0.079	0.431
ALC-3	0.093	0.100	0.988
ALC-4	0.103	0.109	1.540

a range of superficial gas velocities, u_{sg}, from 0.005 to 0.15 m/s. The air sparger was perforated rings made of a 0.8 cm diameter PVC-tubing with 14 orifices (1 mm diameter). The sparger was located at the base of annular section.

3.2. Measurements

3.2.1. Gas holdup

The overall gas holdup, ε_{Go}, was determined by the volume expansion method. The unaerated and aerated liquid heights were measured and ε_{Go} was then calculated from:

$$\varepsilon_{Go} = \frac{H_D - H_L}{H_D} \tag{18}$$

The riser gas holdup, ε_{Gr}, was estimated by measuring the pressure difference, ΔP, between two pressure taps located along the height of the column:

$$\varepsilon_{Gr} = 1 - \frac{\Delta P}{\rho_L g \Delta H} \tag{19}$$

where ΔH is the distance between the two pressure taps.

The riser was assumed to consist of two distinct regions, i.e. up-flow and down-flow regions where gas holdup in the down-flow region, $\varepsilon_{Gr,dn}$, was assumed to be zero. Therefore, $\varepsilon_{Gr,up}$ can subsequently be calculated from:

$$\varepsilon_{Gr,up} A_{r,up} = \varepsilon_{Gr} A_r \tag{20}$$

Downcomer gas holdup, ε_{Gd}, which could not be measured simply by manometer, was calculated from the experimental data of ε_{Go} and ε_{Gr}. It was assumed further that gas holdup in the top section was approximately equal to that in the riser ($\varepsilon_{Gt} = \varepsilon_{Gr}$) and therefore, ε_{Gd} can be computed from:

$$\varepsilon_{Gd} = \frac{\varepsilon_{Go} H_D (A_d + A_r) + (H_{dt} A_d - H_D (A_d + A_r))\varepsilon_{Gr}}{H_{dt} A_d} \tag{21}$$

3.3. Liquid velocity

Liquid velocities both in riser and downcomer were measured using the color tracer technique where the travelling time of color tracer between the two points in the contactor was measured for the calculation of liquid velocity. The lowest pressure tap, 10 cm above the bottom of the airlift column, was employed as an injection point of the color tracer in the riser section. 10 ml of color tracer was slowly injected perpendicularly to the liquid flow direction in the riser, and the detection point was at the top of the draft tube. This allowed the tracer to travel through the entire length of the riser. For the measurement of downcomer liquid velocity, 20 ml of color tracer was injected at the top section above the draft tube. The travelling time was taken as the time required for the tracer to move from the top to the bottom of the draft tube.

4. Results and discussion

4.1. Internal liquid circulation: experimental evidence

Experiments carried out in internal loop ALCs (annulus sparged) showed that, within the range of u_{sg} and A_d/A_r employed in this work, the color tracer in the downcomer moved in a uniform pattern with slight dispersion. Most bubbles were stationary or flowed downwards in downcomer. This implied that the velocity measurement in the downcomer with a color tracer provided reliable results. It was therefore assumed that there was no internal liquid circulation in the downcomer and that the fluid in the downcomer moved uniformly across the cross-sectional area.

On the other hand, large turbulence in the color tracer was observed along the riser section. In addition, liquid velocities measured in the riser and downcomer did not follow the continuity equation (Eq. (1)) where the net liquid flow in riser has to be equal to that in downcomer. Fig. 3 displays the riser liquid velocity (v_{Lr}) measured from the experiment compared with the v_{Lr} computed from Eq. (1) using downcomer liquid velocity (v_{Ld}) from experiments in ALCs with different ratios of downcomer to riser cross-sectional areas (A_d/A_r). The measured v_{Lr} was always observed to have a greater value than the calculated value from Eq. (1) which means that there must exist a down-flow of liquid in the riser to counterbalance the excess liquid up-flow. In other words, an internal liquid circulation must have taken place in the riser of the annulus sparged internal loop ALCs.

4.2. Determination of internal liquid circulation

The simple calculation model based on principals of conservation of mass and energy, i.e. Eqs. (4) and (17), respectively, was employed to estimate the proportion of the internal circulation of liquid in the riser. A proper arrangement of Eqs. (4) and (17) led to two equations with two variables, i.e. liquid velocity in down-flow region of riser ($v_{Lr,dn}$) and area occupied by down-flow region of riser ($A_{r,dn}$). These equations were solved simultaneously using a standard nonlinear iterative procedure to yield $v_{Lr,dn}$ and $A_{r,dn}$. The simulation results are given in the next sections.

4.3. Effect of superficial gas velocity (u_{sg}) on internal liquid circulation

The internal liquid circulation was characterized in terms of up-flow and down-flow liquid fractions in the riser, and

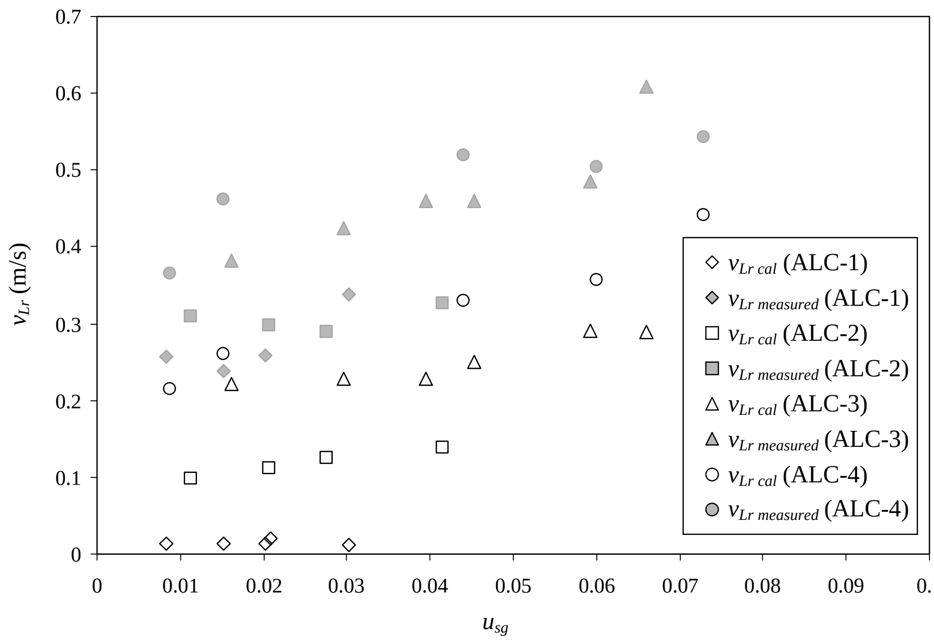

Fig. 3. Comparison between riser liquid velocities calculated from Eq. (1) and from experiments.

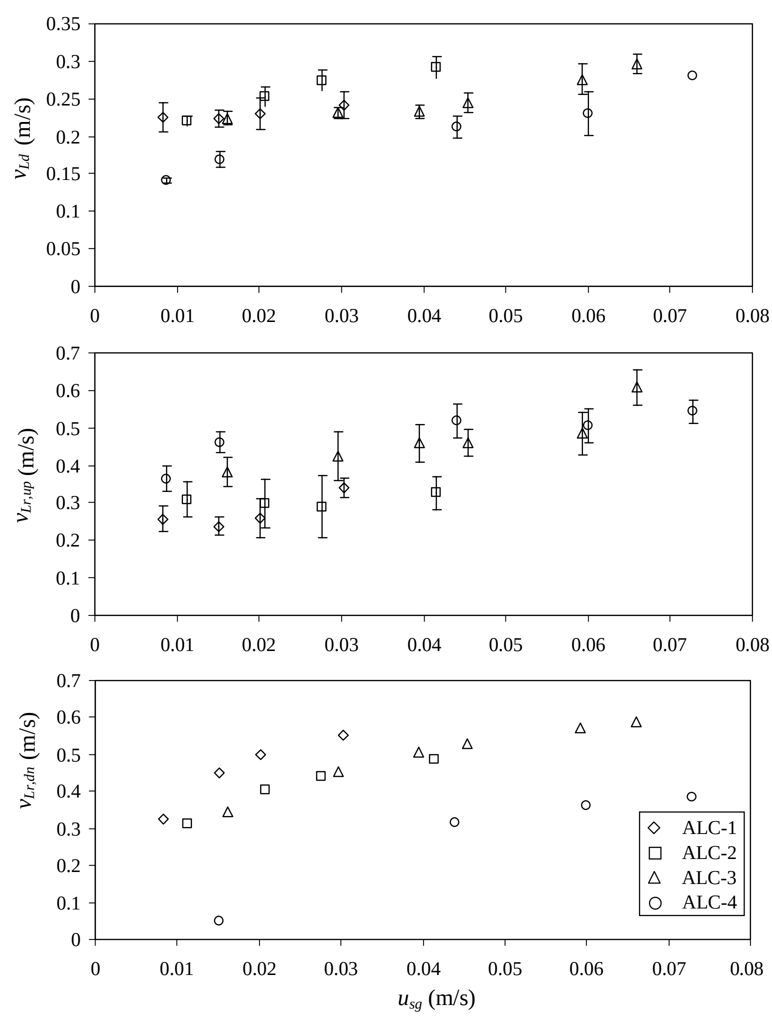

Fig. 4. Experimental data on v_{Ld} and $v_{\mathrm{Lr,up}}$, and simulation results on $v_{\mathrm{Lr,dn}}$ in various ALCs.

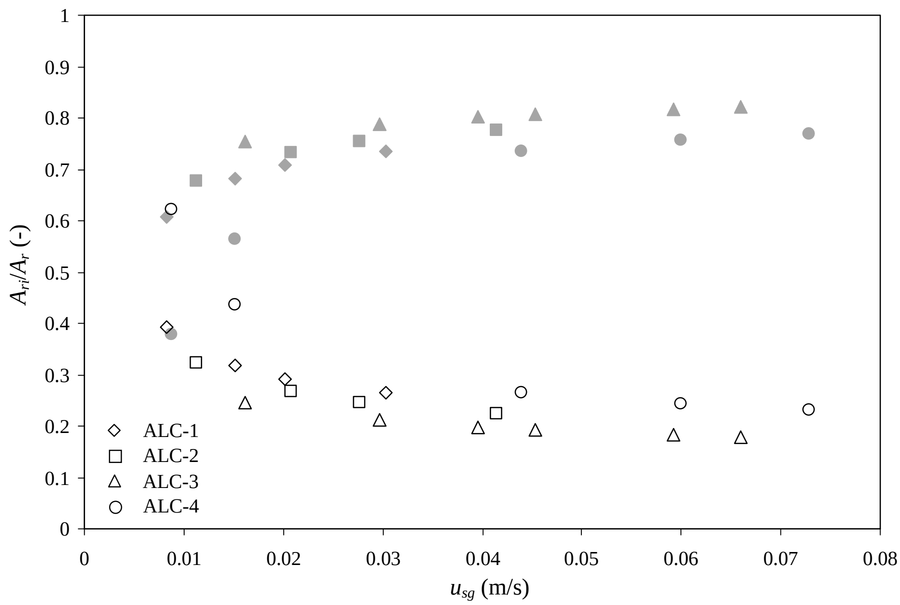

Fig. 5. Up-flow and down-flow area fractions in riser of various ALCs (filled symbols for $A_{r,up}/A_r$ and empty symbols for $A_{r,dn}/A_r$).

this is illustrated in Fig. 4 where experimental results on v_{Ld} and $v_{Lr,up}$ are plotted along with the simulation results on $v_{Lr,dn}$ at various u_{sg} in ALCs with different A_d/A_r. The increase in u_{sg} always resulted in a higher level of both $v_{Lr,up}$ and $v_{Lr,dn}$. The same trend was also found for v_{Ld} for the whole range of u_{sg} employed in this study. This was not unexpected as an increase in gas velocity effectively implied a larger energy input to the system and high liquid velocity was induced. Note that the effect of u_{sg} on $v_{Lr,up}$ was less pronounced than that on $v_{Lr,dn}$, and it is interesting to observe that the down-flow velocity was in many cases higher than the up-flow velocity particularly in the ALC with small A_d/A_r.

The determination of the up-flow and down-flow area fractions resulted in a plot in Fig. 5. The fraction of up-flow area in riser ($A_{r,up}/A_r$) increased steadily with the increase in u_{sg} whilst the opposite was found for the fraction of down-flow area ($A_{r,dn}/A_r$). It was possible that, at low u_{sg}, the behavior the of ALC was close to that of bubble columns where the wall effect played an important role in retarding the movement of the liquid which resulted in a recirculation of liquid within the column. [18] At high u_{sg}, the liquid became highly turbulent which lessened this wall effect and a lower down-flow area was observed.

Information on v_{Lr} and A_r allowed us to determine the volumetric flow rate of liquid up-flow and down-flow in the riser as:

$$Q_{Lr,i} = v_{Lr,i} A_{r,i} (1 - \varepsilon_{Gr,i}) \tag{21}$$

where i = 'up' for up-flow in riser and 'down' for down-flow in riser, and these results are illustrated in Fig. 6.

As stated earlier, despite the high down-flow liquid velocity in the riser, most of the liquid was found to flow upwards as the area for the up-flow was larger than that of the down-flow (see Fig. 5). Interestingly, the proportion of $Q_{Lr,dn}/Q_{Lr,up}$ in each ALC employed in this work was rather constant as shown in Fig. 7. This implied that the ratio between the down-flow and up-flow liquid volumetric flowrates was not affected by the quantity of gas supplied to the system (at least for the range of u_{sg} employed in this work). This information allows one to easily determine the magnitude of the liquid internal circulation within the ALC system.

4.4. *Effect of cross-sectional area ratio between downcomer and riser (A_d/A_r) on internal liquid circulation*

The effect of A_d/A_r on internal liquid circulation can also be extracted from Figs. 4 and 5. Fig. 4 illustrates that there was only a slight effect of A_d/A_r on $v_{Lr,up}$ such that $v_{Lr,up}$ slightly increased with an increase in A_d/A_r. On the other hand, it was apparent that $v_{Lr,dn}$ decreased with an increase in A_d/A_r. The ALC with high A_d/A_r (large downcomer cross-sectional area and small riser) always led to a system with high liquid circulating velocity [19–21]. As the up-flow area (riser) was smaller than the down-flow area (riser + downcomer), increasing A_d/A_r implied that liquid in riser needed to flow with higher velocity to account for the high liquid down-flow. At small A_d/A_r, a relatively low circulating velocity allowed more liquid to flow down in the riser in the same way as the phenomena taken place in bubble columns and a higher down-flow velocity in riser was obtained.

The effect of A_d/A_r on the fraction of areas for up-flow and down-flow in the riser was not detected in this work as elucidated in Fig. 5. The reason for this could not be extracted from this experiment but this information was

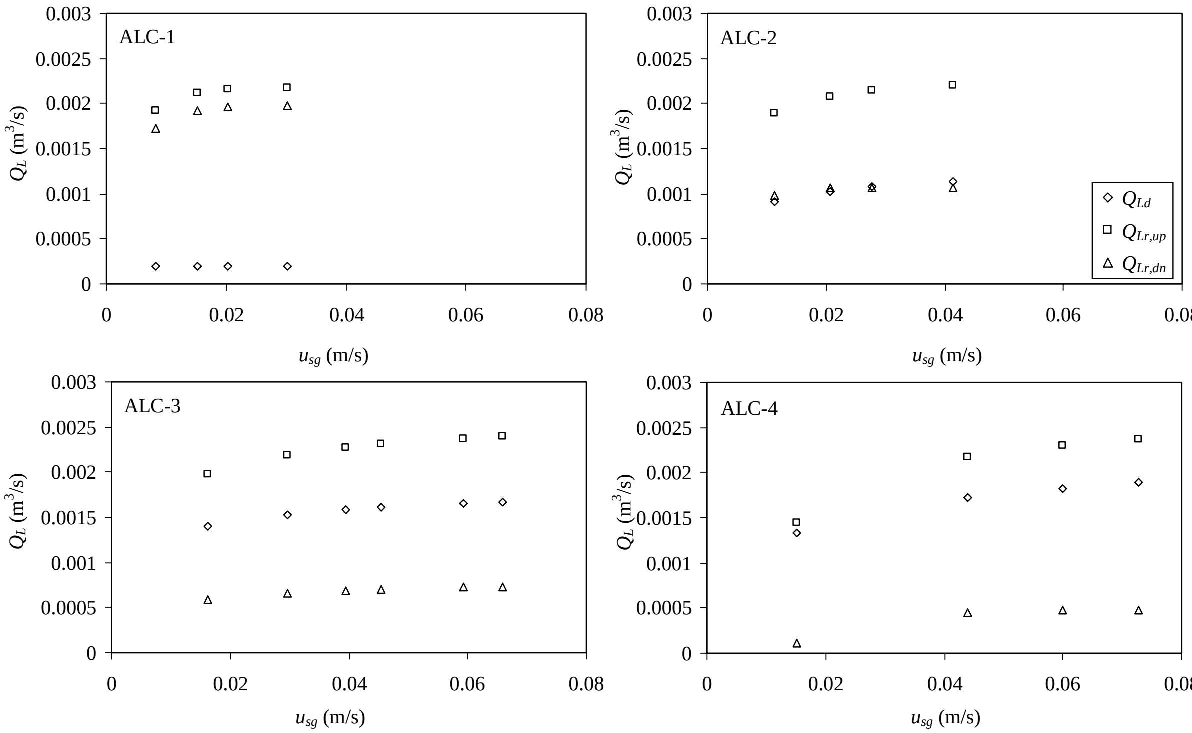

Fig. 6. Liquid volumetric flowrate in various ALCs.

significant as it implied that the down-flow of liquid would always exist in the annulus sparged ALC with a predictable fraction of the total cross-sectional area. However, this fraction of down-flow in the riser depended markedly on u_{sg} as described earlier.

Similar to the discussion in the previous section, the down-flow and up-flow liquid flowrate in riser were calculated based on the information on velocities ($v_{Lr,up}$ and $v_{Lr,dn}$) and cross-sectional areas ($A_{r,up}$ and $A_{r,dn}$) and the results are illustrated in Fig. 6. Fig. 7 demonstrated further

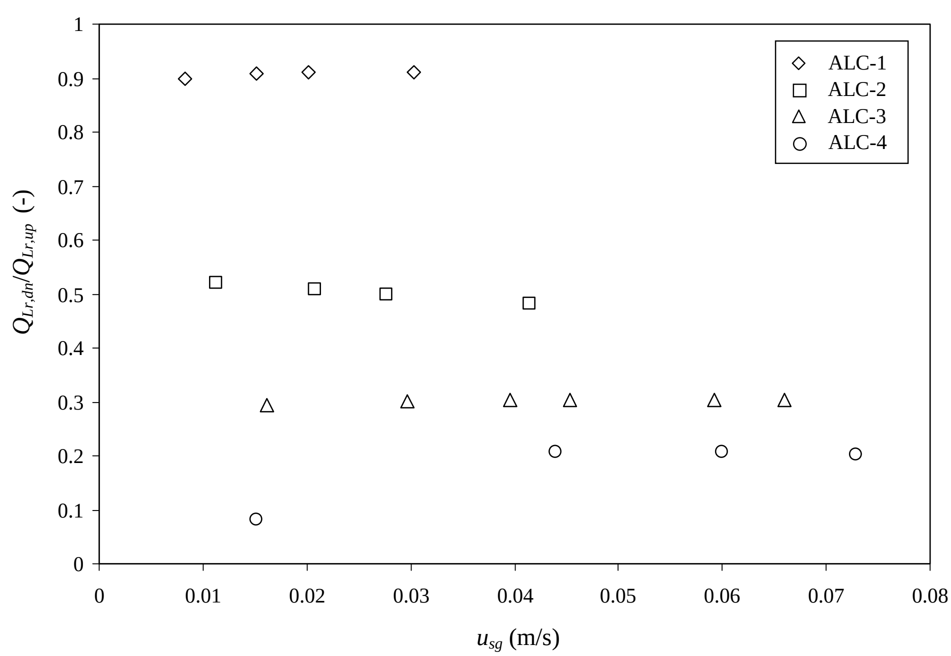

Fig. 7. Fraction of down-flow and up-flow liquid flowrates ($Q_{Lr,dn}/Q_{Lr,up}$) in various ALCs.

that the ratio between the down-flow and up-flow liquid flowrates ($Q_{Lr,dn}/Q_{Lr,up}$) decreased significantly when A_d/A_r increased from 0.067 to 0.988. This is because the configuration of the ALC with an extremely small A_d/A_r (ALC-1) was close to that of bubble column, i.e. large aerated section, and this promoted the internal circulation within the riser. As a result, $Q_{Lr,dn}$ in ALC-1 was almost as great as $Q_{Lr,up}$. As the riser became smaller (larger A_d/A_r), the behavior moved away from the bubble column where the downcomer played a more important role in recirculating liquid. Hence, a smaller extent of internal liquid circulation in riser was obtained and thus a smaller $Q_{Lr,dn}/Q_{Lr,up}$ became more apparent. However, a further increase of A_d/A_r from 0.988 to 1.54 did not seem to have great effect on this liquid flow ratio. Hence, it is concluded that there must exist a critical ratio between downcomer and riser cross-sectional area above which the internal liquid circulation would remain constant, and in this case, this critical A_d/A_r was in the range of 0.988–1.54.

5. Conclusion

This work presented an innovative notion on the determination of the internal liquid circulation in the airlift contacting system. This could be achieved through the combination of experiment and simulation. First, experiments were conducted to reveal that the operation of the airlift contacting system was often subject to the condition where internal liquid circulation existed. Necessary conditions such as up-flow liquid velocity in riser, liquid velocity in downcomer, and gas holdups were also obtained from these experiments. A mathematical calculation based on mass and energy conservations in an annulus sparged airlift contactor was proposed where the magnitude of this internal liquid circulation could then be determined.

Acknowledgements

The authors wish to acknowledge the Thailand Research Fund for their financial support.

References

[1] N. De Never, Bubble driven fluid circulations, AIChE J. 14 (1968) 222–226.
[2] W. Freedman, J.F. Davidson, Hold-up and liquid circulation in bubble columns, Trans. Instit. Chem. Eng. 47 (1969) T251–T262.
[3] J.H. Hills, Radial non-uniformity of velocity and voidage in a bubble columns, Trans. Instit. Chem. Eng. 52 (1974) 1–9.
[4] K. Rietema, Science and technology of dispersed two-phase systems-I and II: I. General aspects, Chem. Eng. Sci. 37 (1982) 1125–1150.
[5] J.-W. Tzeng, R.C. Chen, L.-S. Fan, Visualization of flow characteristics in a 2D bubble column and three-phase fluidized bed, AIChE J. 39 (1993) 733–744.
[6] A.G. Jones, Liquid circulation in a draft-tube bubble column, Chem. Eng. Sci. 40 (1985) 449–462.
[7] J.C. Merchuk, M.H. Siegel, Air-lift reactors in chemical and biological technology, J. Chem. Tech. Biotech. 41 (1988) 105–120.
[8] E.G. Calvo, P. Letón, A fluid dynamic model for bubble columns and airlift reactors, Chem. Eng. Sci. 46 (1991) 2947–2951.
[9] W. Wachi, A.G. Jones, T.P. Elson, Flow dynamics in a draft-tube bubble column using various liquids, Chem. Eng. Sci. 46 (1991) 657–663.
[10] M.J. Lockett, R.D. Kirkpatrick, Ideal bubbly flow and actual flow in bubble columns, Trans. Instit. Chem. Eng. 53 (1975) 267–273.
[11] G.B. Wallis, One-dimensional Two-phase Flow, McGraw-Hill, New York, 1969.
[12] R.B. Bird, W.E. Stewart, E.N. Lightfoot, Transport Phenomena, Wiley, New York, 1960.
[13] J.C. Merchuk, I. Berzin, Distribution of energy dissipation in airlift reactor, Chem. Eng. Sci. 50 (1995) 2225–2233.
[14] H. Kubota, Y. Hosono, K. Fujie, Characteristic evaluations of ICI airlift type deep shaft aerator, J. Chem. Eng. Jpn. 11 (1978) 319–325.
[15] M.Y. Chisti, Airlift Bioreactors, Elsevier Applied Science, London/New York, 1989.
[16] E.G. Calvo, P. Letón, Prediction of gas hold-up and liquid velocity in airlift reactors using two-phase flow friction coefficients, J. Chem. Tech. Biotechnol. 67 (1996) 388–396.
[17] M.Y. Chisti, B. Halard, M.M. Young, Liquid circulation in airlift reactors, Chem. Eng. Sci. 43 (1988) 451–457.
[18] K. Ueyama, T. Miyauchi, Properties of recirculating turbulent two phase flow in as bubble columns, AIChE J. 25 (1979) 258–266.
[19] K. Koide, S. Iwamoto, Y. Takasaka, S. Matsuura, E. Takahashi, M. Kimura, Liquid circulation, gas holdup and pressure drop in bubble column with draught tube, J. Chem. Eng. Jpn. 17 (1984) 611–618.
[20] S.S. Sukan, F. Vardar-Sukan, Mixing performance of airlift fermenters against working volume and draft tube dimension, Bioproc. Eng. 2 (1987) 33–38.
[21] W.A. Al-Masry, A.E. Abasaeed, On the scale-up of external loop airlift reactors: Newtonian systems, Chem. Eng. Sci. 53 (1998) 4085–4094.